NOTICE CONCERNING COPYRIGHT RESTRICTIONS

A NUMERICAL SIMULATION STUDY OF THE OGUNI GEOTHERMAL FIELD

John W. Pritchett

S-Cubed
La Jolla, California, USA

ABSTRACT

The liquid-dominated Oguni geothermal field is located in northeastern Kyushu in Japan. In this paper, a numerical model of the reservoir is presented. The steady "natural" state of the field was described by an unsteady heat-up calculation of 250,000 years duration. Next, the effects of several shallow small-diameter wells which have been operating in the area for the last thirty years were taken into account. The final state of this calculation represents present-day conditions. Comparisons of computed stable reservoir temperatures, pressures, and natural surface discharges with measurements are favorable. Finally, the model was employed in a series of forecasts to estimate the electrical capacity of the field and to design optimum exploitation strategies. These calculations indicate that the Oguni field is capable of supplying 250 tons per hour of steam (separated at 160°C) for more than thirty years.

1. BACKGROUND

The Oguni geothermal prospect (Figure 1) is located in the northern part of the Hohi thermal area in northeastern Kyushu, Japan. The Hohi area (> 200 km^2) also incorporates the operating Hatchobaru/Ohtake geothermal fields (120 MWe) eight kilometers southeast of Oguni. The active Mt. Aso caldera lies twenty kilometers to the south. High upward heat flow prevails throughout Hohi, but only isolated areas are permeable enough to permit hot fluid to rise to shallow depths and form hydrothermal reservoirs (Pritchett and Garg, 1986). Regionally, vertical permeabilities exceed horizontal permeabilities, with average values of horizontal and vertical permeability being around 0.05 and 3 millidarcies, respectively (Pritchett and Garg, 1988). Within the isolated reservoirs, permeabilities are much higher.

During 1979–1985, NEDO (the New Energy and Industrial Technology Development Organization, an agency of the Japanese government) carried out an extensive exploration study of the Hohi area which helped to delineate the Oguni permeable zone. Subsequent NEDO projects have been undertaken to characterize the Hohi system, including the theoretical modeling reported in this paper. The Electric Power Development Company (EPDC) of Tokyo began an ongoing exploration and development program at Oguni in 1983. The government program drilled nine wells in the immediate Oguni area (mostly slim coreholes), and EPDC has drilled more than twenty wells to date (of which many are also slim coreholes) These wells range in depth from 0.5 to 2.6 km (Garg, et. al., 1995).

The local topography is dominated by Mt. Waita, which rises to about 1500 meters above sea level (ASL) southeast of the Oguni borefield. Typically, wellhead elevations are between 750 and 950 m ASL. Drilling in the area has revealed the underlying geological structure in detail. The stratigraphic sequence consists of a series of post-Miocene volcanic flows overlying a Cretaceous granitic basement. The basement forms a nearly horizontal plateau in the southern part of the Oguni field, but dips sharply to the north of the Takenoyu/Hagenoyu hot spring area. To the south, deep wells DW-7 and DY-2 encountered basement at –962 and –1014 m ASL, respectively, but farther north well DY-1 reached –1795 m ASL without finding basement. The basement depth in the Hohi area has been estimated based on regional gravity surveys tied down by occasional drilling encounters, and is not precisely known.

The major formations overlying the basement are (in ascending order), (1) the Pliocene Taio group, (2) the Pliocene/Pleistocene Shishimuta formation, (3) the lower Pleistocene Hohi formation, (4) the middle Pleistocene Kusu group which incorporates sediments and mudstones and interfingers with the Hohi formation to the north, and (5) the late Pleistocene/Recent Kuju volcanics. The Shishimuta and Hohi formations appear to constitute the main geothermal aquifers at Oguni, and the Kuju formation and the Nogami Mudstones (part of the Kusu group) act as caprocks. Surface mapping, drilling logs and geophysical surveys have revealed a series of major WNW-ESE trending faults which pass through the Takenoyu/Hagenoyu hot-spring area. This faulted band is less than 1 km wide. The underlying strata are uplifted relative to rocks to the north and south by ~300 meters.

The reservoir fluid consists of a dilute sodium chloride brine (~0.2% NaCl by mass) with moderate amounts of dissolved CO_2 gas (~0.07%) and other minor constituents (Garg, et. al., 1993). Long-term shut-in temperature surveys are available for many of the wells. Several of these surveys (among them wells GH-4, GH-8, GH-10, GH-11, GH-20, HH-2 and K-7) are nearly

Figure 1. The Oguni geothermal field and immediate environs. Axes: Central Kyushu Coordinate System. Inset map shows the location of the Hohi thermal region (dark rectangle).
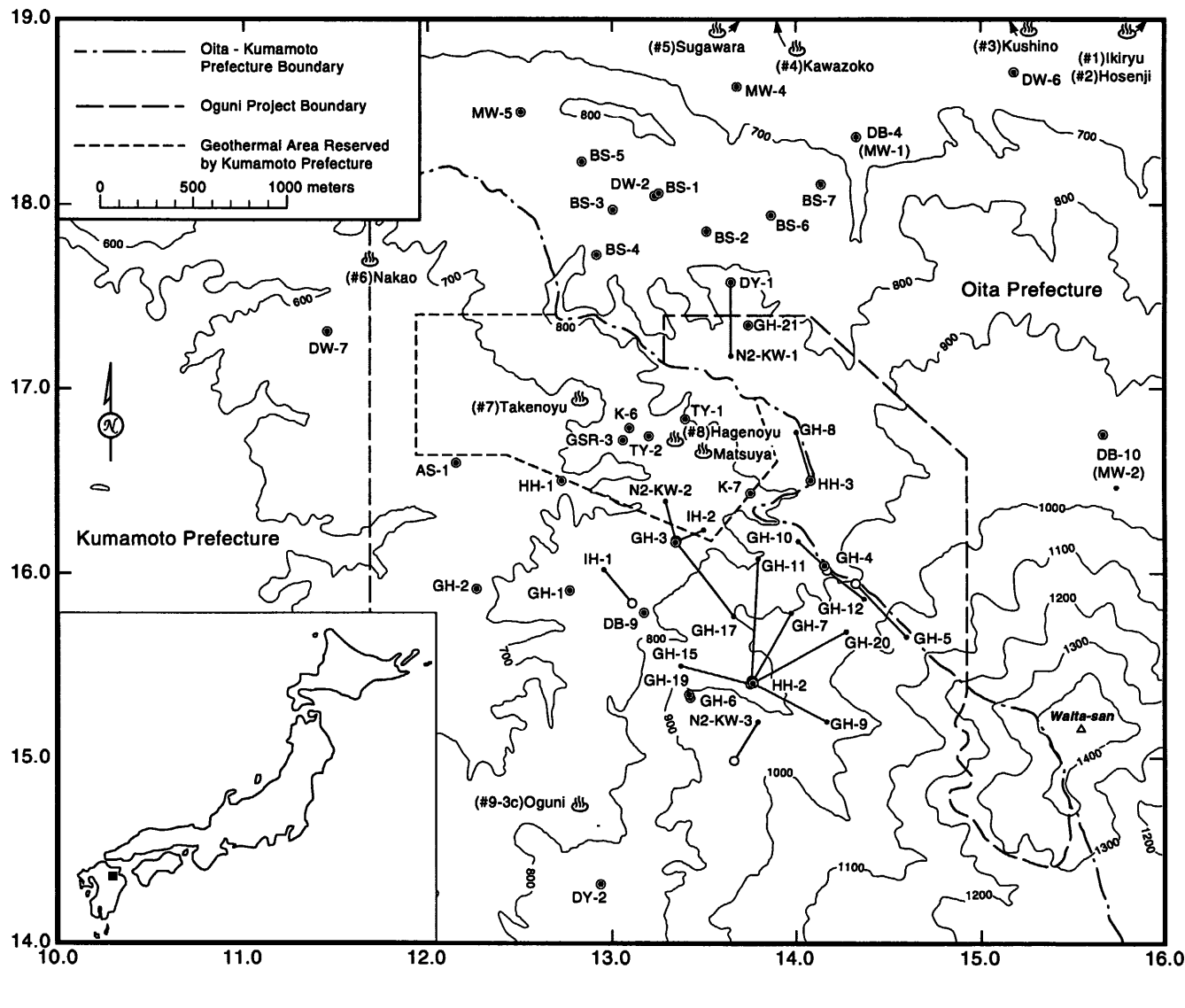
isothermal at depth, indicating fluid upwelling in a crescent-shaped region extending from the western flank of Mount Waita toward the Takenoyu/Hagenoyu hot-spring area. Maximum recorded temperatures in some of these wells exceed 240°C. To the east and north of this central upwelling zone, recorded temperature profiles exhibit pronounced inversions, indicative of buoyant hot fluid outflow in permeable rocks. In the extreme south, little permeability is present—deep well DY-2 exhibits a conductive temperature profile, with a fairly uniform gradient around 60°C/kilometer.

Stable feedpoint pressure values have been established for 39 wells. These reservoir pressure values fall into two distinct classes. Most of the feedpoint pressure determinations may be represented by:

$$P(\text{bars}) = 65.84 - 0.0853\,Z - 0.00065\,N \qquad (1)$$

where Z is feedpoint elevation in meters ASL and N is distance northward in meters (Central Kyushu Coordinate System); the main part of the Oguni borefield lies between 15,000 m $< N <$ 17,000 m. This equation fits the measurements within an RMS tolerance of 0.68 bars. These data imply an average vertical pressure gradient of 85.3 bars/km (hydrostatic for 195°C) and a slight northward pressure decline (0.65 bars per kilometer of distance northward). The elevation of the piezometric surface may be estimated by ex-

trapolating the above equation to one atmosphere pressure; this elevation is +630 m ASL in the Takenoyu/Hagenoyu area and +590 m ASL in the cluster of hot springs (the "Northern Discharge Area") located several kilometers farther north.

A few of the pressure determinations in the southern part of the field (wells GH-6, GH-9, GH-15, GH-19, KW-3 and HH-2) are about nine bars higher than the above correlation suggests. These wells are spatially contiguous, and are the southernmost permeable wells drilled at Oguni. Furthermore, the feedpoints of these "high-pressure" wells all lie in a narrow vertical range between sea level and +200 m ASL. We therefore conclude that there are in fact two separate geothermal aquifers at Oguni—a large, thick "low-pressure" reservoir to the north of well HH-2 which extends to the northernmost wells in the area and beyond, and a relatively small, vertically confined "high-pressure" reservoir to the south.

Pressure interference tests indicate that the reservoir transmissivity is highest (200–250 darcy-meters) in the southern part of the low-pressure reservoir, and is somewhat lower (~100 darcy-meters) north of the Takenoyu/Hagenoyu area. By contrast, the high-pressure zone to the south is much less transmissive (~15 darcy-meters). No pressure interference has ever been observed between "high-pressure" and "low-pressure" wells despite their spatial proximity, but successful interference tests have been performed within each region separately.

In the low-pressure reservoir, hot fluid apparently flows upward from depth below wells GH-4/GH-11/K-7, then flows horizontally toward several hot springs to the extreme north (beyond Figure 1). These hot spring areas collectively discharge around 50 kg/s of hot water—they are all located between 450 and 550 m ASL (slightly below the low-pressure piezometric surface).

In the Takenoyu/Hagenoyu area, numerous hot springs and fumaroles discharge a mixture of hot water and steam (total ~10 kg/s). These features are located at 730 m ASL, above the piezometric surface, which suggests that a two-phase region underlies the Takenoyu/Hagenoyu area which supplies the fluid to the surface by gas-lift. The two-phase region must be relatively shallow, however, since measured deep reservoir temperatures are far below the boiling point at reservoir pressures. Even at 240°C, the bubble-point pressure is only 33.5 bars, corresponding to a depth of 480 meters at Takenoyu/Hagenoyu (according to the above pressure correlation).

The Oguni-Kozan hot spring (~600 m north of well DY-2) may represent the drainage point for the "high-pressure" reservoir—the discharge rate is ~17 kg/s and the elevation is 750 m ASL, which corresponds to the piezometric surface for the high-pressure reservoir. In the high-pressure reservoir, hot fluid appears to flow from east to west.

2. NUMERICAL REPRESENTATION

The general approach was to try to calculate the "natural state" of the Oguni reservoir (using numerical reservoir simula-

tion techniques) starting from "cold" initial conditions and carrying out a lengthy time-dependent calculation until a steady-state was attained. Then, this candidate "natural-state" was compared with measured facts (reservoir pressures, temperatures, hot-spring discharge rates, etc.). Based on these comparisons, appropriate adjustments were made in the various "free parameters" in the model (mainly rock permeabilities, compressibilities, and the boundary conditions imposed on the bottom grid surface) and the long-term calculation was repeated. This cycle continued until an adequate match was attained, which required 28 different "natural-state" computations. Numerical results discussed hereafter pertain to the final case.

The computational volume considered (Figure 2) incorporates all the Oguni wells and extends roughly from well DW-1 in the south to the hot spring area in the north. The surface area is 45 square kilometers. Horizontal grid spacings are 250, 500, 1000 or 2000 meters. Vertically, sixteen layers (each 200 meters thick) are employed, extending from -1900 m ASL to +1300 m ASL. The total grid volume is 144 km³, subdivided into 3,456 grid blocks. Some of the blocks in the upper part of the grid are designated "void" since the ground surface is generally lower than +1300 m ASL. The total number of non-void blocks is 2,878.
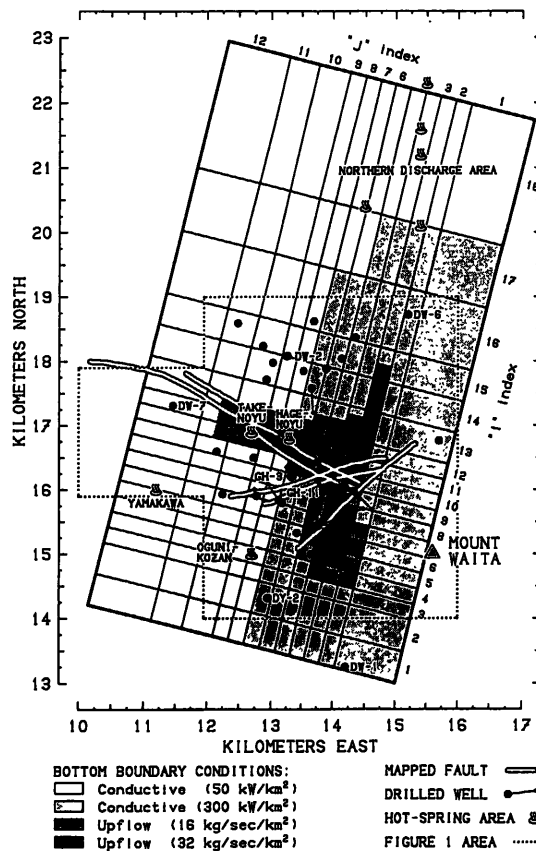

Figure 2. Areal view of the computational grid.

The vertical boundaries of the computing volume (to the north, south, east and west) were treated as impermeable and insulated. At the upper grid surface, a boundary condition of the "fixed-pressure" type was imposed; the location of the one-bar surface (water table) was established based on measured water levels in numerous 80-meter heat flow holes in the area (not shown on Figure 1). The water table is typically 50–80 meters below the local ground surface. Imposition of a fixed-pressure condition on the upper surface allows downward recharge and upward discharge (hot springs, fumaroles) to evolve in a natural fashion. Also, a heat-loss condition was imposed at the ground surface which constrains the temperature in the topmost non-void grid blocks to remain near values implied by the shallow temperature gradients measured in the 80-meter holes. These boundary conditions (on the vertical sides of the computing volume and at the ground surface) remained the same for all 28 attempts to compute the "natural-state".

The boundary conditions imposed on the bottom surface (at −1900 m ASL), on the other hand, were treated as free parameters in the series of 28 calculations and were varied over wide ranges to optimize computed results. The computed temperature distribution is very sensitive to these bottom boundary conditions. The conditions imposed for Case 28 are indicated in Figure 2. Most of the bottom surface was treated as impermeable, but constant-rate conductive heat input was imposed; the prescribed heat flux was 50 kilowatts per square kilometer over the larger part of the area, and 300 kW/km^2 in the southeastern portion near Mt. Waita. Below the Takenoyu/Hagenoyu area and the central part of the Oguni borefield, steady upward mass fluxes were imposed over restricted areas, as indicated. The upflowing fluid was assigned a temperature of 250°C; the total flow imposed was 69.5 kg/s. The total input thermal power supplied from below (relative to 10°C air temperature) is thus 79 MW, of which 8% is conductive and 92% is convective.

For all the natural-state calculations, the initial conditions were hydrostatic with a linear vertical temperature distribution between 150°C at −1900 m ASL to air temperature (10°C) at the ground surface. Since the "natural-state" is essentially steady, the exact initial conditions are unimportant.

Drilling logs were used to guide the assignment of different rock formations to the various grid blocks. Figure 3 shows how the various major formations were assigned in the north-south
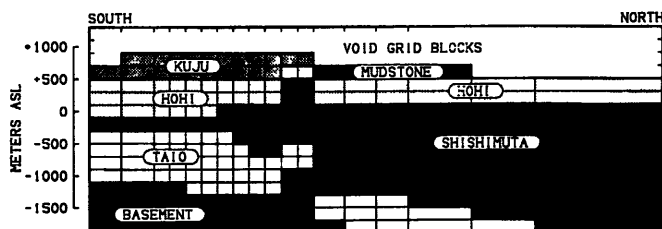

Figure 3. Assignment of rock formations to grid blocks in north-south vertical plane "$j = 5$".

section at "$j = 5$". Several of the pertinent rock properties were obtained by averaging results of laboratory core sample analyses:

Formation	Grain Density (g/cm^3)	Porosity	Grain Heat Capacity (J/g/°C)	Grain Thermal Conductivity (W/m/°C)
Kuju Volcanics	2.46	0.12	0.93	1.87
Kusu/Mudstone	2.60	0.19	0.90	3.01
Hohi Formation	2.65	0.11	0.91	2.25
Shishimuta	2.45	0.11	0.92	2.60
Taio Group	2.50	0.07	0.92	2.25
Basement	2.74	0.01	0.86	3.33

Furthermore, it was assumed that, within the small two-phase region, capillary effects could be neglected and that the relative permeability to each flowing phase (water, steam) was equal to the saturation (pore volume fraction) of the phase. Clearly, virtually all the large-scale permeability at Oguni arises from an intricate fracture network (laboratory tests indicate that small core samples have no interstitial permeability), but the fracture spacing is small enough to permit treatment of the entire reservoir as a porous medium on the time/space scales of interest.

The remaining important rock properties are the absolute permeability and elastic modulus. These properties were established as a part of the "free parameter" variation process during the 28 natural-state calculations, using results from pressure-transient testing as a guide. It was found that many of the rock formations were non-uniform in permeability; final values (Case 28) are:

Formation	Elastic Modulus (kilobars)	Permeability Range (md) Horizontal	Permeability Range (md) Vertical
Kuju Volcanics	0.8	0.05 md	0.05 to 3 md
Kusu/Mudstone	80	0.05 md	0.05 md
Hohi Formation	80	0.05 to 200 md	3 to 20 md
Shishimuta	8	0.05 to 200 md	3 to 20 md
Taio Group	8	0.05 to 200 md	3 to 20 md
Basement	80	0.05 md	3 md

Figure 4 illustrates the distribution of vertically-integrated "horizontal permeability-thickness product" over the study area, obtained from the final permeability distributions adopted to best match field data. The region of highest permeability corresponds to the Takenoyu/Hagenoyu uplift zone; permeabilities are somewhat lower (but still substantial) farther north. The isolated region of moderate permeability to the south is the "high-pressure reservoir" discussed above. These transmissivity values are consistent with interference-test results.

3. CALCULATION OF THE NATURAL STATE

Most of the calculation of the "natural state" (the situation prior to human intervention) was carried out using the NIGHTS

HORIZONTAL PERMEABILITY-THICKNESS PRODUCT: $\int (k_x k_y)^{1/2} dz$

☐ BELOW 10 DARCY-METERS
▨ 10 TO 25 DARCY-METERS
▦ 25 TO 75 DARCY-METERS
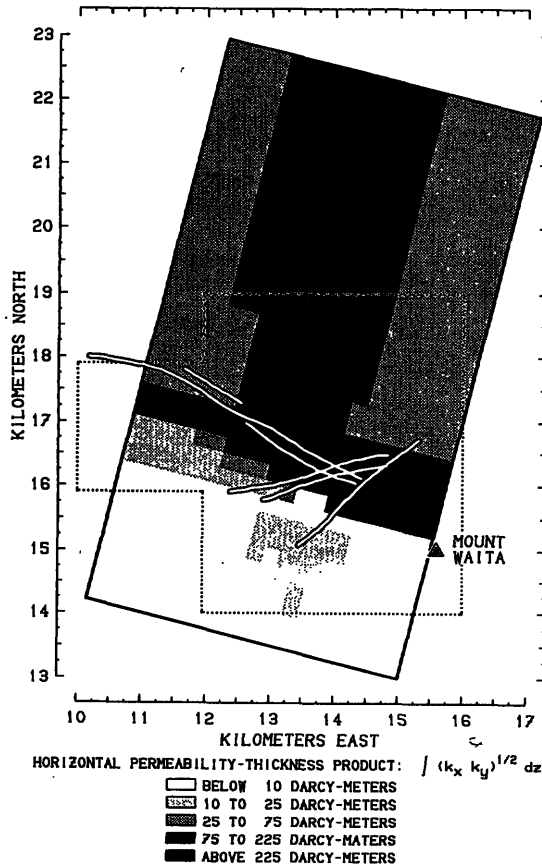▪ 75 TO 225 DARCY-MATERS
■ ABOVE 225 DARCY-METERS

Figure 4. Distribution of permeability-thickness product in final model.

reservoir simulator (Pritchett, 1995a). NIGHTS is restricted to single-phase liquid fluid flow, but has significant advantages in computational speed. Figure 5 shows the change in total grid thermal energy with time (relative to the initial state) during the 250,000 year calculation. The time-step size employed was 25 years. Actually, this calculation was carried out twice as far as really necessary—changes during the last 100,000 years or so were negligible.
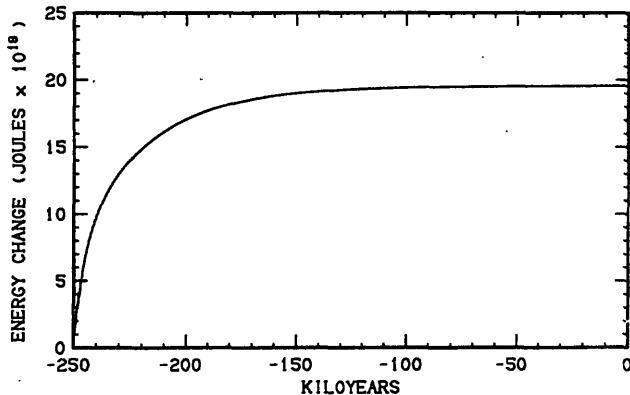

Figure 5. NIGHTS natural-state calculation.

Underground temperatures and pressures obtained after 250,000 years compare favorably with measured values, but 16 grid blocks (all above +300 m ASL, in the Takenoyu/Hagenoyu area) were characterized by computed temperatures in excess of the boiling point for the local grid block pressure. This is the area where, in reality, two-phase flow is taking place (see above). NIGHTS treats the region as all-liquid, so the NIGHTS description in this part of the system is inadequate.

To take the two-phase region into account, the STAR general-purpose multiphase geothermal reservoir simulator (Pritchett, 1995b) was used. The STAR simulation employed exactly the same grid block spacings, formation properties and boundary conditions as the preceding NIGHTS calculation. Initial conditions (pressure and temperature) for each STAR grid block were taken as the final values computed by NIGHTS, except in the 16 grid blocks mentioned above. In those grid blocks, the initial pressure was adjusted upward, so as to just exceed the bubble-point pressure for the local temperature. Therefore, all grid blocks initially contained single-phase liquid, but the 16 overpressured blocks quickly decompressed, forming a two-phase region. The STAR calculation used a time-step of 1/32 year, and was carried forward 6,000 years. The total steam volume in the grid rose from zero to ~ 13 million cubic meters in the first ten years, declined to a minimum near 5 million cubic meters after 60 years, then began to increase again slowly. Finally, a steady condition was again attained after 6,000 years (see Figure 6); the equilibrium total steam volume is 13.2 million cubic meters. Outside the immediate neighborhood of the two-phase region, changes in computed reservoir temperatures were negligible throughout the entire 6,000-year computed history. Re-stabilization of the system is much more rapid (6,000 years) than was required to establish the natural state using NIGHTS (> 100,000 years) since the volume of the two-phase zone is small in comparison with the overall grid volume.
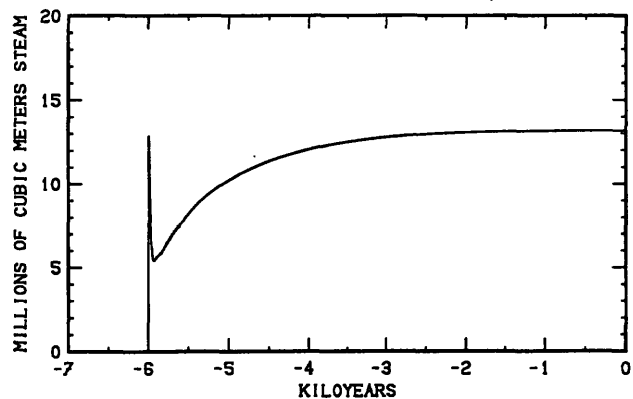

Figure 6. STAR calculation—development and stabilization of the two-phase region.

4. CALCULATION OF THE PRESENT STATE

The resulting natural-state is characterized by substantial upflows and downflows of fluid at the ground surface. The total

fluid discharge rate (over the entire upper surface) was 92.9 kg/s, with three-fourths of the natural discharge in the extreme northern part of the grid. This upflow was accompanied by 23.4 kg/s of downward cold-water recharge through the surface, mainly in the eastern part of the system near Mt. Waita. Smaller discharges were indicated in the Takenoyu/Hagenoyu area (8 kg/s) and near Oguni-Kozan (15 kg/s). Figure 7 illustrates the general spatial distribution of calculated natural-state fluid upflow and downflow at the ground surface. It is noteworthy that all observed natural discharge areas fall within the regions for which the numerical model predicts fluid upflow at the surface.
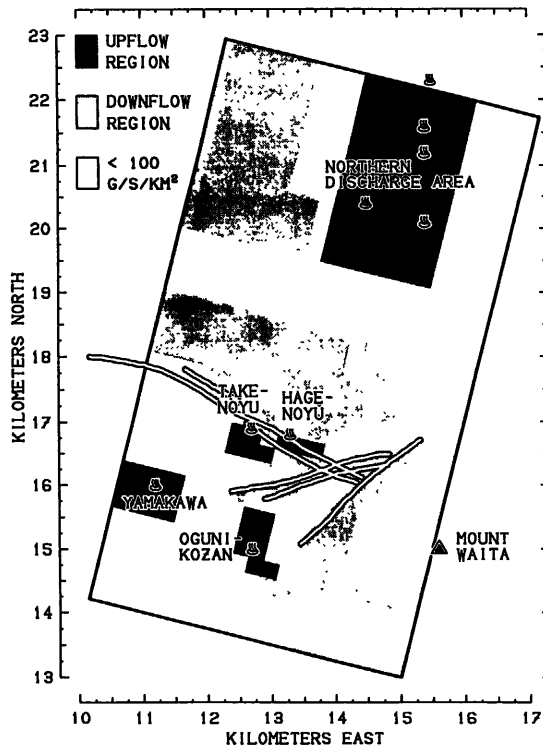

Figure 7. Areas of computed natural-state fluid upflow and downflow at the ground surface.

Since World War II, local hot-spring resort operators have drilled several shallow small-diameter wells to augment and control hot water flows. In aggregate, these shallow wells represent a significant fraction (~30%) of the presently-observed surface discharge. Unfortunately, the operational histories of the shallow wells are not well-documented. To estimate the effects which these operations have had on the "natural state", we assumed (1) that all such shallow wells started operating simultaneously 30 years ago, and (2) that since that time each well discharged at a constant rate, equal to the rate reported during the 1979-1985 government survey of the Hohi area. Total reported discharge from these shallow wells amounts to 23.7 kg/s.

The shallow wells were next incorporated in the STAR simulation and the calculation was carried forward another 30 years, using a time-step size of 1/64 year. The situation at the end

of the calculation was taken to represent the "present state" of the Oguni reservoir. Figure 8 shows that one effect of the operation of these shallow wells was to slightly increase the size of the two-phase region, owing to induced reservoir pressure decline (roughly one bar after 30 years in the deep part of the main Oguni wellfield). No significant changes in reservoir temperature were observed. Note that, as an experiment, the calculation was also carried forward 30 years into the future (Figure 8). Thirty years is too short a time for a new state of equilibrium to become established, so that the "present state" of the Oguni field is not entirely steady, but rates of change are generally small for practical purposes.
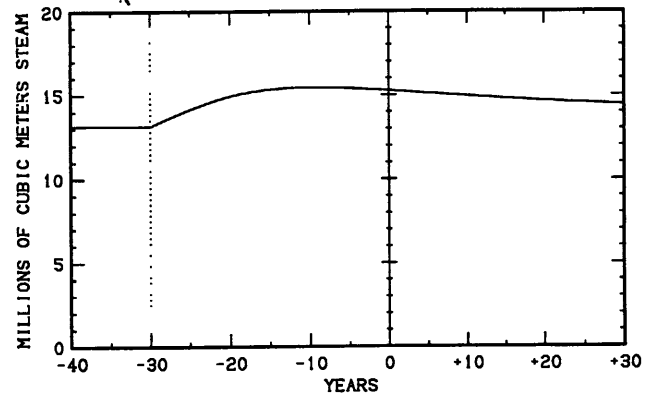

Figure 8. Effects of shallow-well operations on the two-phase region.

The remaining spontaneous surface discharges (natural discharge apart from shallow wells) were, however, significantly reduced by the operation of these wells. Total computed spontaneous discharge declined from 92.9 kg/s to 77.5 kg/s, although the total discharge (spontaneous flow plus that from the shallow wells) increased from 92.9 to 101.2 kg/s. Virtually all (99.7%) of the computed discharge in the "present state" takes place within the identified "hot spring" areas; the "northern discharge area" (Kabeyu, Ikiryu, Hosenji, Kushino and Kawazoko), the Takenoyu/Hagenoyu area, Yamakawa, and Oguni-Kozan. Computed total discharges compare with reported values as follows:

	Computed Total Discharge (kg/s)	Reported Total Discharge (kg/s)	Shallow Wells (kg/s)
Northern Area	70.9	47.5	14.7
Takenoyu/Hagenoyu	11.6	9.4	5.1
Yamakawa	3.9	3.9	3.9
Oguni-Kozan	14.6	17.3	0
Entire Grid Area	101.2	78.1	23.7

In view of the substantial uncertainties in the reported values (and the possibility of unreported discharges) these comparisons are considered adequate.

Figure 9 shows how the measured stable shut-in feedpoint pressures in the various Oguni wells compare with values interpo-

lated among principal grid-block pressures to the location of each well's feedpoint. On the average, the computed values are high by 0.5 bars (one standard deviation is ±1.2 bars). If only the wells in the low-pressure region are considered, the comparison is even better (average deviation 0.3 bars high ±0.9 bars). These deviations are comparable to the uncertainties in the measured pressures themselves, most of which were computed based on measured shut-in standing water levels and temperature profiles.
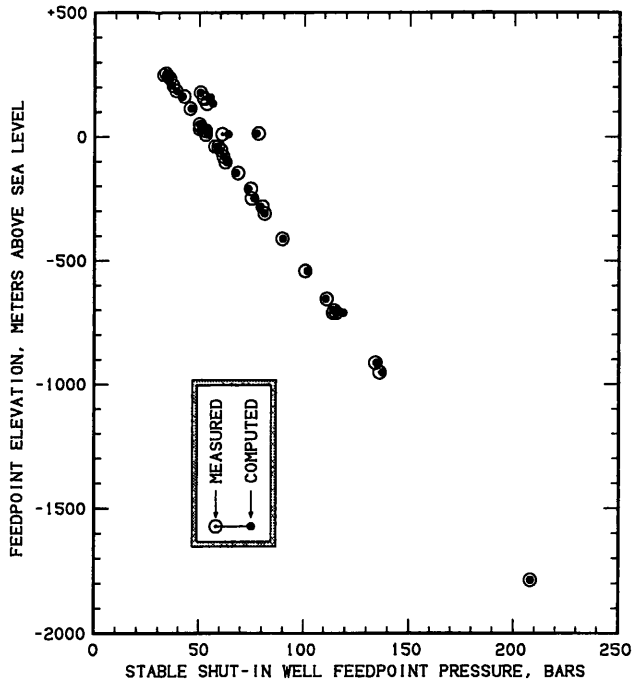

Figure 9. Comparison of measured and computed reservoir pressures.

Between December 1991 and April 1992, EPDC carried out a large-scale flow test which involved producing fluid from "low-pressure" wells GH-10, GH-11, GH-12 and GH-20. The separated brine was reinjected into "low-pressure" wells GH-17, IH-1 and IH-2 and "high-pressure" wells GH-15 and GH-19. Capillary-tube downhole pressure gauges were installed in shut-in wells KW-1 (~1 km north of the flowing wells) and KW-3 (in the "high-pressure" reservoir). We simulated this experiment by using the "present state" as starting conditions and imposing the measured flow rate histories in the production and injection wells. Figure 10 shows the computed pressure histories interpolated to the feedpoint locations of the observation wells compared to the recorded pressure signals. Although the high-frequency features of the signals are not well-reproduced in the computed response (owing largely to the fact that the spatial separation between the flowing wells and the observation wells is only 2-3 grid blocks), on the whole the comparison is reasonably satisfactory.

Long-term shut-in downhole temperature profiles from 36 different wells were available for comparison with the computed "present" temperature distribution (by interpolating computed grid temperatures along the well track). A representative sample of these comparisons is shown in Figure 11. Locations of these wells are
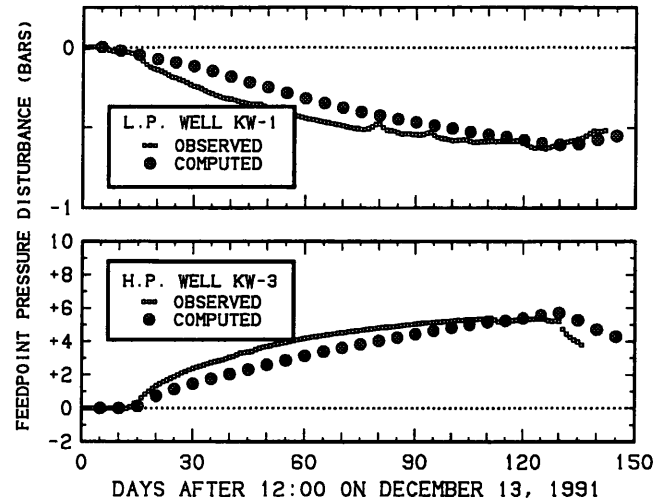

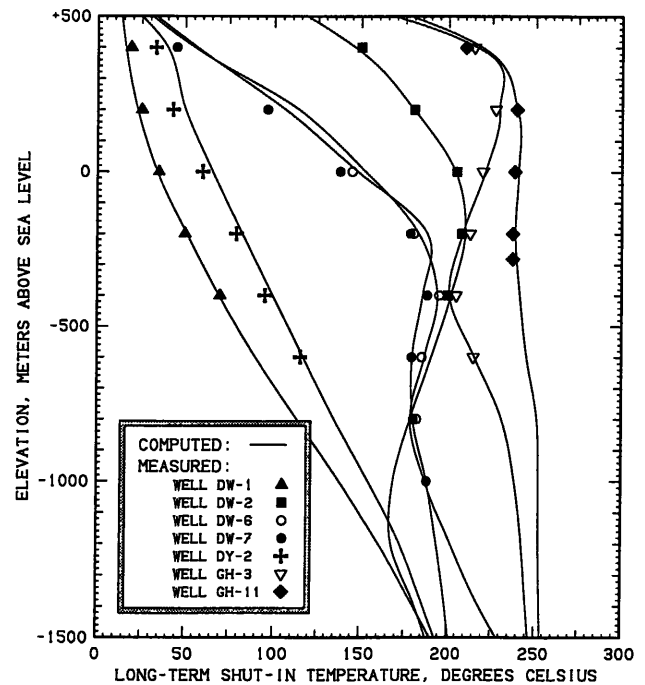Figure 10. Pressure interference results from the 1991/1992 flow test.

Figure 11. Selected comparisons between downhole shut-in stable temperature profiles in wells and computed "present" reservoir temperature distribution.

indicated in Figure 2. Well DY-2 (as discussed above) is impermeable/conductive, located to the south of the Oguni borefield. Well DW-1 is characterized by cold-water downflow above sea level, and is impermeable (conductive) at greater depths. Wells DW-7 (northwest of the borefield), DW-2 (to the north), DW-6 (northeast) and GH-3 (in the eastern part of the main drilled area) all exhibit temperature inversions characteristic of outflow zones. Well GH-11 is located in the middle of the Oguni upflow area, and has a nearly uniform temperature profile.

5. PERFORMANCE FORECASTS

Once a satisfactory representation of the present state of the Oguni reservoir had been developed, we proceeded to carry out a series of parametric forecasts of the probable response of the field to fluid production for electrical power generation. For all of these forecasts, the properties of the rocks and the boundary conditions were maintained the same as in the prior "natural-state" and "present-state" calculations. The shallow wells associated with the hot-spring resorts, moreover, were assumed to continue to withdraw fluid at the same rates as before. To simulate the exploitation of the Oguni field, additional deep production and injection wells were incorporated into the model at various locations. The forecasts all extend 30 years into the future, and employed a time-step size of 1/64 year.

In all cases, we assumed that the production and injection wells are all of uniform inside diameter (22.44 cm). Flowing well-head pressure for all production wells was maintained at or above 6.86 bars (absolute). Each production well was assumed to have a time-dependent productivity index given by:

$$PI = V^*/v \qquad (2)$$

where v is the time-dependent flowing kinematic viscosity of the fluid in the grid block containing the well feedpoint, and V^* is a constant with dimensions of volume. A similar treatment is employed for the injectivity indices of the injection wells. For these calculations, we assumed that all wells are characterized by the same value of V^*, obtained by consideration of productivity index data obtained from full-size production wells in the Oguni field:

Well	PI (kg/s/bar)	$V^*(m^3)$
GH-10	3.88	5.31×10^{-12}
GH-11	5.65	7.81×10^{-12}
GH-12	5.77	8.15×10^{-12}
GH-20	15.22	20.82×10^{-12}
IH-2	11.89	17.14×10^{-12}
Arithmetic Mean:		11.84×10^{-12}
Geometric Mean:		10.38×10^{-12}

For most cases, we assumed that V^* would be equal to 11×10^{-12} m^3 for all production and injection wells. It was assumed that steam is separated at 6.18 bars (160°C). Separated steam is passed through a single stage turbogenerator; 35% of the steam is assumed to remain as excess condensate (at 20°C) which is mixed with the separated brine (under pressure) and reinjected.

The model operates in a "fixed steam flowrate" mode; if, at any instant of time, the capacity of the wellfield to supply steam is insufficient, an additional make-up well is automatically "drilled". Similarly, we assumed that the maximum injection well-head pressure is given by the separator pressure, so that if injection pressures rise above this level the simulator will automatically "drill" another injection well. The simulator is provided ini-

tially with a list of candidate "production wells" and "injection wells", which are employed as needed (in a prescribed order) to maintain the desired steam flow rate through the turbogenerator.

A typical case involves the production of steam at a constant rate of 250 metric tons per hour using production wells in the low-pressure "production area" with waste brine injected in the "injection area" as illustrated in Figure 12. Feedpoints of the production wells vary from +200 m ASL to -200 m ASL; the injection well feedpoints are presumed to lie between sea level and -200 m ASL. The particular order in which specific wells were "drilled" was selected randomly. Figure 13 illustrates the changes induced in the reservoir by this case after 30 years. Note particularly the injection-induced cooling of the reservoir and the expansion in size of the two-phase region due to reservoir pressure decline. The average production borefield reservoir pressure decreases by around seven bars in this case, and the total reservoir volume occupied by steam triples. Figure 14 illustrates the well drilling requirements to maintain 250 tons/hour of steam; at early times, eight production wells and four injection wells suffice, but by 30 years, twelve production wells and five injection wells are needed.

Several calculations were carried out to establish the sensitivity of the computed results to certain key assumptions. First, we ran cases in which the productivity index parameter V^* (above)
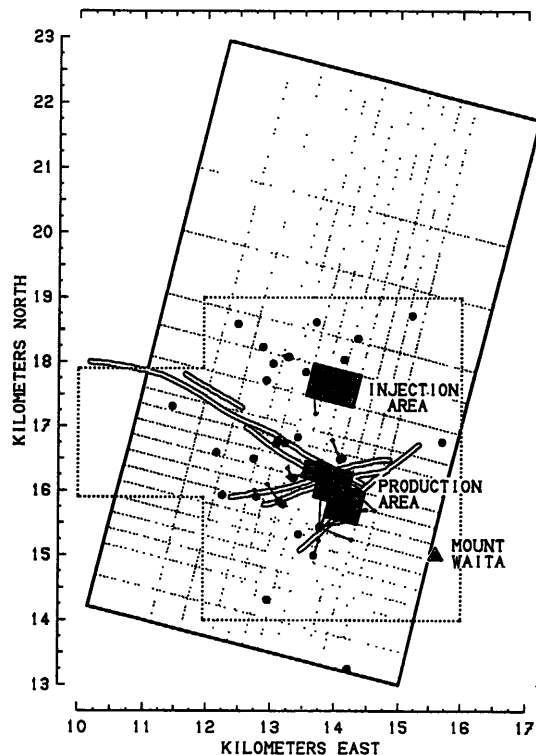

Figure 12. Locations of fluid production and injection wells for typical exploitation case.
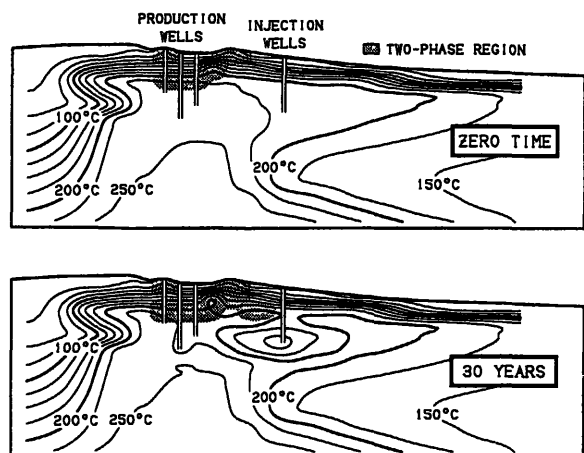
Figure 13. Changes in underground conditions in north-south vertical section "*j* = 5" after 30 years for typical case (250 tons/hour of steam). Contour interval is 25°C.
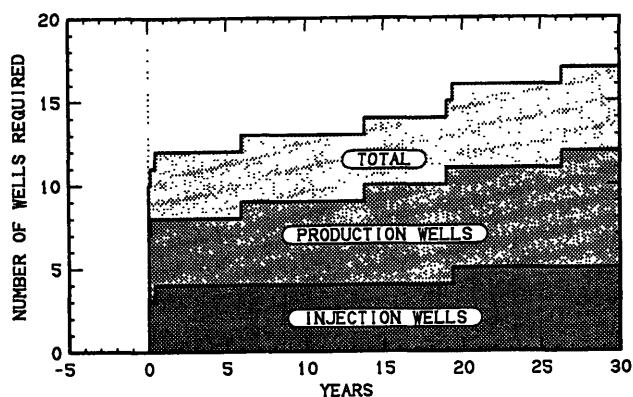

Figure 14. Drilling requirements for typical case.

was assumed to be both smaller and larger than the "standard" value (11×10^{-12} m³). Varying V^* by over a factor of two changes the average well drilling requirements by less than 10%. The reason is that productivity indices and reservoir permeabilities are so high at Oguni that the main restriction on well performance is pipe friction, not reservoir resistance. Also, as noted above, a particular (random) order was assumed in which the various production and injection wells are "drilled". Several cases were run in which this order was randomly permuted. The variations in well drilling requirements were less than 10% among the various cases, again because of the high reservoir permeability; if the permeability is sufficient, the exact locations of the wells are not very important.

Other parametric calculations were carried out to appraise various locations for the injection wellfield and to assess the maximum practical steam delivery capacity (250 tons/hour is near the practical limit). Other schemes were also evaluated, such as the

desirability of attempting fluid production from the "high-pressure reservoir". Computed results indicate that, owing to its limited transmissivity and small volume, no more than one or two production wells should be sited in the high-pressure area for optimum overall reservoir performance.

6. CONCLUDING REMARKS

A numerical model has been constructed for the Oguni geothermal field which is internally consistent, conservative in character, and in good agreement with available measurements from the field. Calculations based upon the model indicate that the Oguni field is capable of delivering sufficient steam for a moderate-size geothermal power plant for thirty years or more. EPDC is now planning the construction of a geothermal power station to exploit the steam from the field for the generation of electrical power.

7. ACKNOWLEDGEMENTS

The numerical simulation study reported in this paper was supported primarily by NEDO. The authors wish to express their gratitude to EPDC for their generous cooperation in releasing proprietary reservoir data for publication in this paper.

8. REFERENCES

Garg, S. K., J. W. Pritchett, T. G. Barker, L. A. Owusu, J. Haizlip and A. H. Truesdell (1993), "Reservoir Engineering Studies of the Oguni Geothermal Field (Phase 3)", S-Cubed, La Jolla, California, Report SSS-R-92-13899.

Garg. S. K., J, Combs and M. Abe (1995), "A Study of Production/Injection Data from Slim Holes and Large-Diameter Production Wells at the Oguni Geothermal Field, Japan", World Geothermal Congress 1995, Florence, Italy.

Pritchett, J. W. and S. K. Garg (1986), "Geothermal Reservoir Engineering Study of the Hohi Area, Kyushu Island, Japan: A Summary", S-Cubed, La Jolla, California, Report SSS-R-86-7858.

Pritchett, J. W. and S. K. Garg (1988), "An Analytical Model for Estimating Terrain Influence on Reservoir Pressures—Implications for Hohi Thermal Area", *Proc. International Symposium of Geothermal Energy 1988: Exploration and Development of Geothermal Resources*, pp. 236-239, Kumamoto/Beppu, Japan.

Pritchett, J. W. (1995a), "NIGHTS: A Single-Phase Geothermal Reservoir Simulator", World Geothermal Congress 1995, Florence, Italy.

Pritchett, J. W. (1995b), "STAR: A Geothermal Reservoir Simulation System", World Geothermal Congress 1995, Florence, Italy.